

Article

Oxidation of 5-Hydroxymethylfurfural on Supported Ag, Au, Pd and Bimetallic Pd-Au Catalysts: Effect of the Support

Dmitrii German ¹, Ekaterina Pakrieva ^{1,2}, Ekaterina Kolobova ¹, Sónia A. C. Carabineiro ^{3,4}, Marta Stucchi ⁵, Alberto Villa ⁵, Laura Prati ⁵, Nina Bogdanchikova ⁶, Vicente Cortés Corberán ² and Alexey Pestryakov ^{1,*}

- ¹ Research School of Chemistry & Applied Biomedical Sciences, National Research Tomsk Polytechnic University, Lenin Av. 30, 634050 Tomsk, Russia; germandmitry93@gmail.com (D.G.); epakrieva@mail.ru (E.P.); ekaterina_kolobova@mail.ru (E.K.)
- ² Instituto de Catálisis y Petroleoquímica, Consejo Superior de Investigaciones Científicas, Marie Curie 2, 28049 Madrid, Spain; vcortes@icp.csic.es
- ³ Centro de Química Estrutural, Instituto Superior Técnico, Universidade de Lisboa, Av. Rovisco Pais, 1049-001 Lisbon, Portugal; sonia.carabineiro@fct.unl.pt
- ⁴ LAQV-REQUIMTE, Department of Chemistry, NOVA School of Science and Technology, Universidade NOVA de Lisboa, 2829-516 Caparica, Portugal
- ⁵ Dipartimento di Chimica, Università degli Studi di Milano, via Camillo Golgi 19, 20133 Milano, Italy; marta.stucchi@unimi.it (M.S.); Alberto.Villa@unimi.it (A.V.); laura.prati@unimi.it (L.P.)
- ⁶ Centro de Nanociencias y Nanotecnología, Universidad Nacional Autónoma de México, 22800 Ensenada, Mexico; nina@cnyunam.mx
- * Correspondence: pestryakov2005@yandex.ru



Citation: German, D.; Pakrieva, E.; Kolobova, E.; Carabineiro, S.A.C.; Stucchi, M.; Villa, A.; Prati, L.; Bogdanchikova, N.; Cortés Corberán, V.; Pestryakov, A. Oxidation of 5-Hydroxymethylfurfural on Supported Ag, Au, Pd and Bimetallic Pd-Au Catalysts: Effect of the Support. *Catalysts* **2021**, *11*, 115. <https://doi.org/10.3390/catal11010115>

Received: 19 December 2020

Accepted: 11 January 2021

Published: 14 January 2021

Publisher's Note: MDPI stays neutral with regard to jurisdictional claims in published maps and institutional affiliations.



Copyright: © 2021 by the authors. Licensee MDPI, Basel, Switzerland. This article is an open access article distributed under the terms and conditions of the Creative Commons Attribution (CC BY) license (<https://creativecommons.org/licenses/by/4.0/>).

Abstract: Oxidation of 5-hydroxymethylfurfural (HMF), a major feedstock derived from waste/fresh biomass, into 2,5-furandicarboxylic acid (FDCA) is an important transformation for the production of biodegradable plastics. Herein, we investigated the effect of the support (unmodified and modified titania, commercial alumina, and untreated and treated Sibunit carbon) of mono- and bimetallic catalysts based on noble metals (Ag, Au, Pd) on selective HMF oxidation with molecular oxygen to FDCA under mild and basic reaction conditions. The higher selectivity to FDCA was obtained when metals were supported on Sibunit carbon (Cp). The order of noble metal in terms of catalyst selectivity was: Ag < Au < Pd < PdAu. Finally, FDCA production on the most efficient PdAu NPs catalysts supported on Sibunit depended on the treatment applied to this carbon support in the order: PdAu/Cp < PdAu/Cp-HNO₃ < PdAu/Cp-NH₄OH. These bimetallic catalysts were characterized by nitrogen adsorption-desorption, inductively coupled plasma atomic emission spectroscopy, high resolution transmission electron microscopy, energy dispersive spectroscopy, X-ray diffraction, Hammett indicator method and X-ray photoelectron spectroscopy. The functionalization of Sibunit surface by HNO₃ and NH₄OH led to a change in the contribution of the active states of Pd and Au due to promotion effect of N-doping and, as a consequence, to higher FDCA production. HMF oxidation catalyzed by bimetallic catalysts is a structure sensitive reaction.

Keywords: gold; silver; palladium; nanoparticles; metal oxides; Sibunit carbon; support modification; bimetallic catalysts; 5-hydroxymethylfurfural; selective oxidation; 2,5-furandicarboxylic acid

1. Introduction

The unavoidable predicted depletion of fossil resources determines the need to develop methods for using new and renewable sources. Nowadays, biomass, a valuable source of energy, along with biological and chemical raw materials, can be a real alternative to obtain biofuels and chemicals. Carbohydrates are the basis of biomass (up to 75%) [1]. Their dehydration into furan derivatives is one of the most intensively developed approaches to biomass transformation [2].

Among them, 5-hydroxymethylfurfural (HMF), produced by fructose or glucose dehydration [3], is considered as a key reagent. It is called a “platform compound” for the

production of a variety of practically important products, including polymers, pharmaceuticals, solvents and fuels [4].

2,5-furandicarboxylic acid (FDCA) is one of the most important chemicals obtained from HMF. It can be potentially used as a precursor for the production of polyethylenefuranoate (PEF), biopolyester, designed to replace the oil-derived polyethylene terephthalate (PET). Furthermore, FDCA has been identified by the US Department of Energy as 1 of 12 priority bio-based chemicals for a green chemical industry [5]. FDCA is commonly synthesized through oxidation of HMF, even though using stoichiometric inorganic oxidants, along with harmful solvents or non-recyclable homogeneous catalysts, under harsh conditions [6–8]. Development of heterogeneous catalysts that are able to use air or molecular oxygen as oxidant and water as solvent is considered a green alternative and more promising for industrial implementation.

Supported catalysts based on noble metals (Pd, Pt, Ru or Au) [9–14] or their combination (bimetallic systems) [15–18] have demonstrated high activity and selectivity for HMF oxidation. However, their catalytic activity is strongly sensitive to many factors, such as metal dispersion, preparation method, nature of the support, metal-support interaction, etc. Additionally, the presence of an alkaline medium is necessary to promote the catalytic activity and assure the solubility of the products formed. Davis et al. [19] suggested that OH^- from solution facilitates the formation of geminal diols (intermediate) from aldehyde and water for further oxidative dehydrogenation (by adsorbed $-\text{OH}$ groups on the surface of metal) to the final FDCA. At the same time, the produced FDCA is neutralized by bases, or else it would adsorb strongly on the metallic centers, thus leading to deactivation. Therefore, this research topic still requires further investigation.

The present work aims to study the effect of the support (unmodified and modified TiO_2 , alumina materials, and functionalized and non-functionalized carbon) for mono- and bimetallic catalysts based on noble metals (Ag, Au, Pd) for FDCA synthesis from HMF oxidation, under basic mild conditions ($60\text{ }^\circ\text{C}$, H_2O as solvent, 3 bar O_2). The parameters determining the performance of the most active catalysts, in particular, support modification, will be discussed as well.

2. Results and Discussion

2.1. Catalytic Results

Table 1 presents screening of Au-, Ag-, Pd-based and PdAu heterogeneous catalysts for aqueous liquid phase oxidation of HMF under the reaction conditions reported in previous studies (0.15 M HMF, HMF/metal: 200 mol/mol, $60\text{ }^\circ\text{C}$, 3 bar O_2 , 2 equiv. NaOH, 2 h) [17,18].

In this reaction, the synthesis of FDCA, derived from the oxidation of both carbonyl and hydroxyl groups, proceeds through intermediate 5-hydroxymethyl-2-furancarboxylic acid (HFCA) formation, obtained by oxidation of the aldehyde group (Scheme 1).

The screening started with previously investigated catalysts: Au supported on unmodified and modified titania ($\text{M}_x\text{O}_y/\text{TiO}_2$) materials used for aerobic liquid phase oxidation of different type of alcohols: n-octanol, glycerol and betulin, under mild conditions [20–23]. Briefly, the best catalytic performance among Au catalysts supported on modified titania were reached with catalysts modified with lanthanum oxide ($\text{Au}/\text{La}_2\text{O}_3/\text{TiO}_2$), regardless of the alcohol type studied [20–23]. In addition, recently obtained results in betulin oxidation using Au/Alumina catalysts revealed that Au/AlOOH-C catalyst is superior to $\text{Au}/\text{La}_2\text{O}_3/\text{TiO}_2$ in both activity and selectivity [24].

However, catalytic systems based on titanium oxide (Table 1, entries 3–7) as well as various aluminum materials (Table 1, entries 8–10) have shown the same level of performance in FDCA production. This is clearly demonstrated on $\text{Au}/\text{La}_2\text{O}_3/\text{TiO}_2$ and Au/AlOOH-C: 11 and 10% of FDCA selectivity after 2 h (Table 1, entries 5 and 8). Thus, despite the various properties (structural, textural, electronic, etc.) of the studied gold catalysts, these systems were little effective in the formation of FDCA. Nevertheless, the

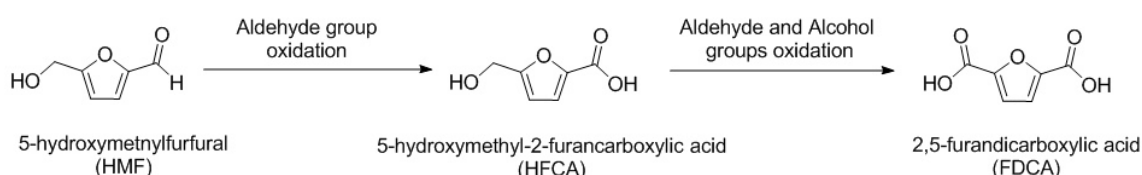
highest selectivity towards FDCA (20%) was achieved on Au/AlOOH-S (Table 1, Entry 10). Carbon balance was 95–100% in all cases.

Table 1. Catalytic behavior of supported Ag, Au, Pd and PdAu NPs on different materials for HMF oxidation under basic conditions ^a.

Entry	Catalyst	Conversion, % After 2 h	Selectivity, %		Carbon Balance, %
			HFCA	FDCA	
1	No catalyst	0	0	0	100
2	No catalyst + NaOH	30 ^b	100	0	31
3	Au/TiO ₂	97	94	6	95
4	Au/Fe ₂ O ₃ /TiO ₂	98	93	7	95
5	Au/La ₂ O ₃ /TiO ₂	99	89	11	95
6	Au/MgO/TiO ₂	99	87	13	95
7	Au/CeO ₂ /TiO ₂	99	84	16	96
8	Au/AlOOH-C	99	90	10	95
9	Au/Al ₂ O ₃ -V	100	88	12	95
10	Au/AlOOH-S	100	80	20	95
11	Ag/CeO ₂ /TiO ₂	36	100	0	30
12	Pd/AlOOH-S	97	50	50	100
13	Ag/Cp	98	98	2	69
14	Au/Cp	100	79	21	95
15	Pd/Cp	99	45	55	97
16	PdAu/Cp	99	40 (28) ^c	60 (72)	100 (98)
17	PdAu/Cp-HNO ₃	99	35 (25)	65 (75)	96 (96)
18	PdAu/Cp- NH ₄ OH	99	30 (18)	70 (82)	98 (95)

^a—Reaction conditions: 0.15 M 5-hydroxymethylfurfural (HMF) (H₂O, 0.15 L), NaOH/HMF = 2 equiv., p(O₂) = 3 atm, T = 60 °C, R = 200;

^b—data after 5 h; ^c—data after 6 h in brackets; HFCA—5-hydroxymethyl-2-furancarboxylic acid; FDCA—2,5-furandicarboxylic acid.



Scheme 1. Detected products from aqueous HMF oxidation over supported Au, Pd and PdAu catalysts under basic conditions.

Ag/CeO₂/TiO₂, the most active catalyst for betulin and n-octanol oxidation among Ag/M_xO_y/TiO₂ (M = Ce, Fe, Mg) catalysts [25], was also examined for HMF oxidation (Table 1, Entry 11). This Ag catalyst was less active in terms of both conversion and FDCA formation. Only 36% of HMF was converted to HFCA and some unidentified byproducts were detected after 2 h of reaction. It explains the low carbon balance, comparable to the results in the blank experiments under basic conditions (Table 1, Entry 2). According to literature [12,26], these unknown substances are polymeric products (humins) formed from degradation of HMF, unstable in basic solution. Nevertheless, in the presence of an active catalyst, HMF can be rapidly converted to the oxidized intermediates because the high catalyzed reaction rate surpasses the degradation. Thus, it is important to design a highly active catalyst able to rapidly oxidize HMF before its thermal polymerization in basic solution, because no reaction occurred in the absence of NaOH (Table 1, Entry 1).

Many studies and reviews [14,27] have shown that Pd catalysts are more selective towards FDCA formation at low temperatures, while Au catalysts tend to be applied at high temperatures and base concentrations and much longer reaction time for higher

performances. For this reason, Pd was loaded on the AlOOH-S, since Au on this support exhibited the highest performance to produce FDCA among Au-catalysts tested. 2.5-fold FDCA yield (50%) was achieved on Pd/AlOOH-S (Table 1, Entry 12), in comparison to its Au/AlOOH-S counterpart.

As the reached yields of FDCA (target product) were not satisfactory, the following step was to look for more effective supports for the noble metals.

There are a large number of examples indicating the higher activity of catalysts on carbon supports compared to oxides. Carbon supports are characterized by a high specific surface area, a developed porous space to transfer of reactants and reaction products, controlled chemical surface properties and chemical inertness, especially in the environment of strong acids and bases [28–30].

In this study, commercial graphite-like Siberian carbon with mesoporous structure, called Sibunit, obtained by matrix synthesis technology [30], was used for this purpose. Sibunit material, which combines the properties of graphite (strength characteristics, corrosion resistance) and active carbons (developed surface, etc.), is a suitable support for catalysts for liquid-phase oxidation processes [31–33].

Thus, single noble metals (Ag, Au and Pd) were deposited by a sol-immobilization method on Sibunit (Cp), and examined for HMF oxidation under the same conditions described above. The order of FDCA formation in this case was: Ag/Cp < Au/Cp < Pd/Cp (Table 1, entries 13–15). At the same time, in comparison to Ag/CeO₂/TiO₂, enhanced activity (98% of conversion) and selectivity (2% of FDCA) were observed for Ag/Cp, although carbon balance was still worse but at higher level (69%) than for Ag/CeO₂/TiO₂. Meanwhile, Au/Cp showed almost the same catalytic properties, when comparing to the most active among all gold catalysts, i.e., Au/AlOOH-S. Finally, slightly higher selectivity to FDCA ($S_{\text{FDCA}} = 55\%$) was obtained on Pd/Cp catalyst, in comparison to Pd/AlOOH-S ($S_{\text{FDCA}} = 50\%$). Nevertheless, it should be mentioned that the highest FDCA selectivity was achieved when metals (Ag, Au or Pd) were supported on Sibunit carbon.

It is well known that a well-designed binary noble metal system, with an optimal composition, can exhibit performance superior to those of the corresponding monometallic catalysts for many catalytic reactions, thus showing a synergistic effect. In addition, several studies [14,34,35] revealed that Au catalysts are more active for the oxidation of aldehyde groups, namely the first step of the oxidation reaction (HMF to HFCA), whereas Pd catalysts are more active for the oxidation of alcohol groups. Thus, the final step in finding the most selective catalyst for FDCA formation was the use of bimetallic systems—depositing the combination of palladium and gold (since silver-based catalyst showed lower activity and did not successfully compete with HMF degradation) on the best support found for noble metals, i.e., Sibunit. As expected, FDCA selectivity (60%) was increased when PdAu/Cp was used (Table 1, Entry 18), compared to both monometallic Pd/Cp ($S_{\text{FDCA}} = 55\%$) and Au/Cp ($S_{\text{FDCA}} = 21\%$).

Catalytic properties of nanodispersed metals deposited on carbon materials depend significantly on the support pretreatment. It is difficult to stabilize metal NPs on the carbon support due to its chemical inertness. Therefore, preliminary treatment of carbon is required before its interaction with precursors, in order to increase the carbon reactivity, i.e., to enhance the interaction between the active phase and the support [28–30]. For this reason, Sibunit support was treated with 20 wt.% solution of nitric acid and ammonium hydroxide (denoted as Cp-HNO₃ and Cp-NH₄OH, respectively) and the bimetallic catalysts obtained were investigated for HMF oxidation. As expected, after 2 h, the modified catalysts produced 5 and 10% FDCA more than the non-treated PdAu/Cp analogues (Table 1, entries 16 to 18). Moreover, this beneficial effect of both treatments can be clearly seen at the initial catalytic activity, i.e., after just 15 min of reaction 1.3-fold and 2-fold FDCA yield were obtained on PdAu/Cp-HNO₃ and PdAu/Cp-NH₄OH, respectively, in comparison to untreated PdAu/Cp (Table 2).

Table 2. Activity of Pd-Au/Sibunit catalysts with different treatment of support in HMF oxidation ^a.

Entry	Catalyst	Conversion, % After 15 min	Selectivity, %		Yield, %		Carbon Balance, %
			HFCA	FDCA	HFCA	FDCA	
1	PdAu/Cp	83	69	31	57	26	100
2	PdAu/Cp-HNO ₃	80	57	43	46	34	100
3	PdAu/Cp-NH ₄ OH	93	38	62	31	52	95

^a—Reaction conditions: 0.15 M HMF (H₂O, 0.15 L), NaOH/HMF = 2 equiv., p(O₂) 3 atm, T = 60 °C, R = 200.

On the basis of these promising results, we explored the performance of bimetallic catalysts with longer run times, up to 6 h. Thus, results show obvious enhancement of catalytic activity, as expected (Table 1, Figures 1 and 2). In particular, the following order of support treatment was found in terms of FDCA formation (S_{FDCA} , %): PdAu/Cp < PdAu/Cp-HNO₃ < PdAu/Cp-NH₄OH. As it should be noted, 100% conversion and 95–98% carbon balance were observed in all cases.

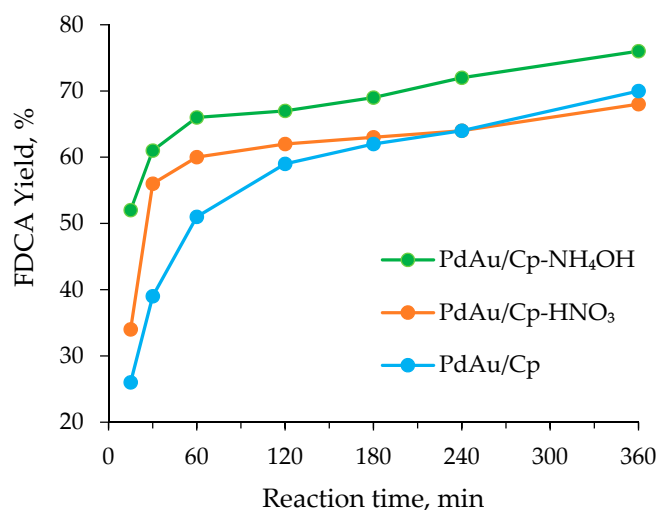


Figure 1. Effect of Sibunit support treatment on the oxidation of HMF on Pd-Au catalysts: evolution of FDCA yield with run time. Reaction conditions: 0.15 M HMF (H₂O, 0.15 L), NaOH/HMF = 2 equiv., T = 60 °C, p(O₂) 3 atm, R = 200.

Thus, the results obtained demonstrate a positive effect of the treatment of Sibunit, especially with NH₄OH, for FDCA production. In this work the maximum FDCA yield ($Y_{FDCA} = 76\%$) was obtained on PdAu/Cp-NH₄OH after 6 h. At the same time, partial deactivation with run time was observed in case of PdAu/Cp-HNO₃ catalyst (Figure 1).

In order to reveal the main factors responsible for the remarkable catalytic properties exhibited by these bimetallic systems and, notably, the effect of Sibunit treatment, a series of physicochemical studies were carried out for these dual noble metal samples.

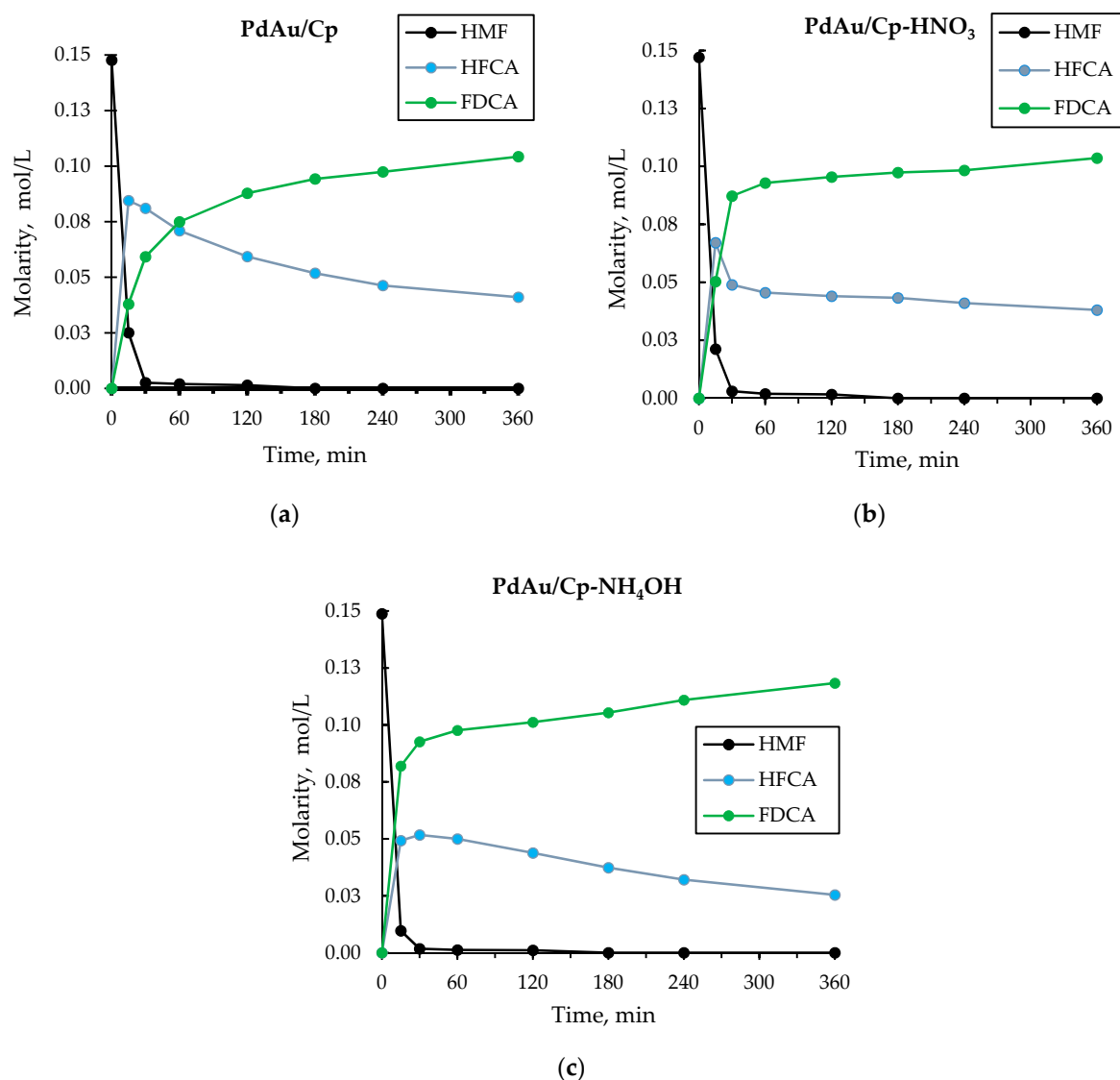


Figure 2. Product distributions in HMF oxidation on gold supported catalysts (a–c). Reaction conditions as in Figure 1.

2.2. Catalyst Characterization

According to the data presented in Table 3, the specific surface area (S_{BET}) of Sibunit supports increased by 17% and 13%, as result of modification with HNO₃ and NH₄OH, respectively (Table 3, entries 1–3). PdAu/Cp is characterized by a higher S_{BET} (by 14%) and an increase in the pore volume (by 20%), when compared to the corresponding support. This is possibly due to the removal of the amorphous phase or the formation of additional defects on Sibunit under H₂SO₄ adding to immobilize metal nanoparticles on the support. At the same time, deposition of two metals on both modified supports did not lead to significant changes, which can be related with the removal of the amorphous phase or the formation of additional defects during treatment of Sibunit with HNO₃ or NH₄OH. N₂ isotherms for all studied carbon-based materials are of type II, with H3 type hysteresis, indicating adsorption in multilayers, as in mesoporous materials with slit-like shaped pores (Figure S1). Thus, in general, the textural properties of three catalysts do not differ significantly from each other (Table 3, entries 4–6).

Table 3. Textural properties of catalysts and their corresponding Sibunit supports.

Entry	Sample	BET Surface Area, m ² g ⁻¹	Pore Volume, cm ³ /g	Pore Size, nm
1	Cp	281	0.48	6.1
2	Cp-HNO ₃	329	0.62	6.7
3	Cp-NH ₄ OH	318	0.58	6.4
4	PdAu/Cp	327	0.60	6.4
5	PdAu/Cp-HNO ₃	313	0.58	6.5
6	PdAu/Cp-NH ₄ OH	331	0.62	6.5

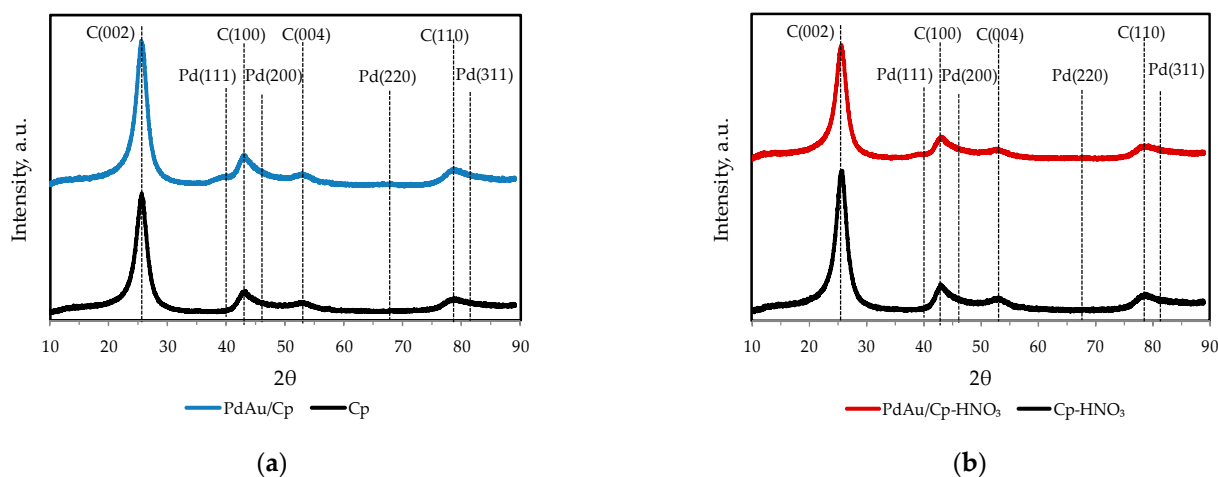
Elemental analysis (Table 4) showed that deposition of Pd and Au on unmodified Sibunit was close to the nominal values; however, Pd and Au were loaded on both modified Sibunit samples in lower amounts: 23% and 40% less than the nominal values, respectively. This probably can be related to the changing of the point of zero charge (PZC) due to the modification of Sibunit, which led to incomplete deposition of the bimetallic colloid. Thus, total Pd-Au content in modified Sibunit samples was 24% less than on PdAu/Cp.

Table 4. Analytical content of Pd and Au in Sibunit-supported catalysts with different support treatment.

Element Content	PdAu/Cp	PdAu/Cp-HNO ₃	PdAu/Cp-NH ₄ OH
Pd, wt.%	0.73	0.57	0.56
Au, wt.%	0.32	0.19	0.20

XRD analysis of catalysts and their corresponding supports (Figure 3) showed no alteration in the phase composition or the support structure after bimetallic system loading. Besides that, no peaks related to Pd or Au were found, indicating either the small size of the Pd and Au particles or their X-ray amorphous structure. Diffraction lines belonging to the support ($2\theta = 25.7, 44.3, 54, 78$) correspond to graphite with a hexagonal lattice, in agreement with the literature data [36,37].

Figure 4 displays the size distribution of bimetallic Pd-Au particles on Sibunit surface, as well as the corresponding HRTEM images. The size range of Pd-Au NPs on unmodified Sibunit was from 3 to 8 nm, and the average particle size (D_m) 3.9 nm (Figure 4a). Modification of Sibunit with HNO₃ or NH₄OH did not lead to significant changes in the distribution of bimetallic particles and their average size. Thus, D_m of PdAu/Cp-NH₄OH was 4.0 nm with a 2–8 nm range (Figure 4c), while PdAu/Cp-HNO₃ showed slightly larger particles in the range of 3–10 nm with an average size of 4.2 nm (Figure 4b).

**Figure 3.** Cont.

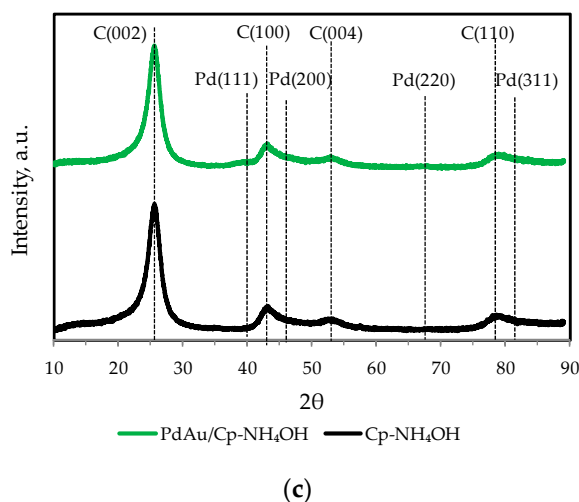


Figure 3. XRD patterns for catalysts PdAu/Cp (a), PdAu/Cp-HNO₃ (b) and PdAu/Cp-NH₄OH (c) and their corresponding supports.

XPS was used to study the electronic state of palladium, gold, oxygen, carbon and nitrogen in the studied bimetallic systems (Figure 5).

Analysis of Pd3d spectra (Figure 5a–c) showed that palladium was present on the surface of all catalysts in three states: Pd⁰, Pd²⁺ and Pd⁴⁺ with binding energies (BE) (Pd3d_{5/2}) 335.9–336.1, 337.7–337.8 and 338.7 eV, respectively [38–41]. The binding energies attributed in this study to Pd⁰, 335.9 and 336.0 eV, exceed the standard BE value characterizing the Pd⁰ state (335.4 eV) by 0.5 and 0.6 eV, respectively. It shows the presence of highly dispersed metal particles on the surface of the studied samples, which shifts binding energies towards higher values up to 1 eV [42–45]. The contribution of the electronic states of palladium found on the surface of the investigated catalysts is presented in Table 5. As can be seen, the distribution among the various states of palladium was approximately the same for the three investigated catalysts. The total surface concentration of palladium was practically the same for all samples (Table 6).

Gold was on the surface of all catalysts in two states, Au⁰ and Au⁺, with BE (Au4f_{7/2}) 84.1–84.2 and 85.2–85.4 eV, respectively (Figure 5d–f). The ratio between these states changed slightly upon Sibunit surface modification (Table 5). However, the largest contribution of monovalent gold was found for PdAu/Cp-NH₄OH. At the same time, the surface concentration of gold was the same (0.3 at.%) for both modified catalysts, while the untreated sample showed a slightly higher gold content (Table 6). These results of gold and palladium surface concentration were in line with the lower metal content after their deposition on treated Sibunit supports found by elemental analysis (Table 4).

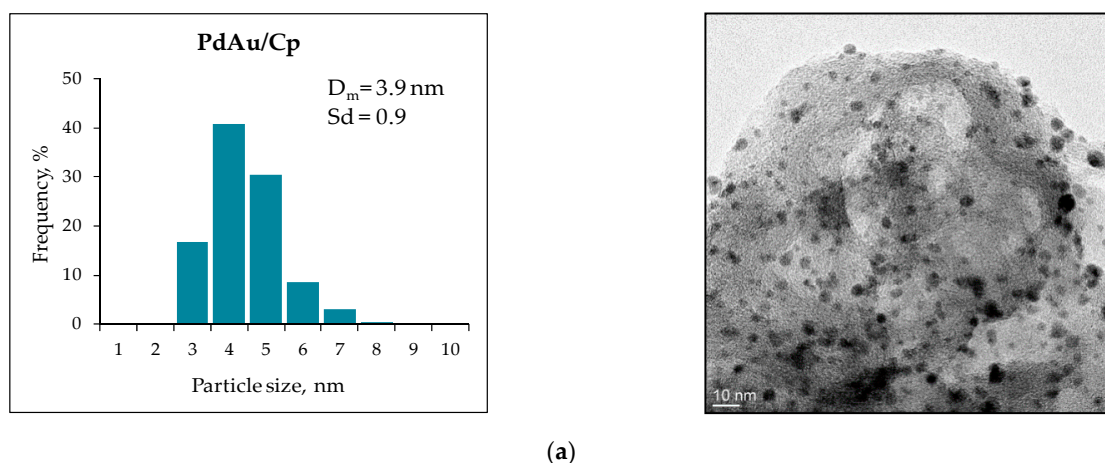


Figure 4. Cont.

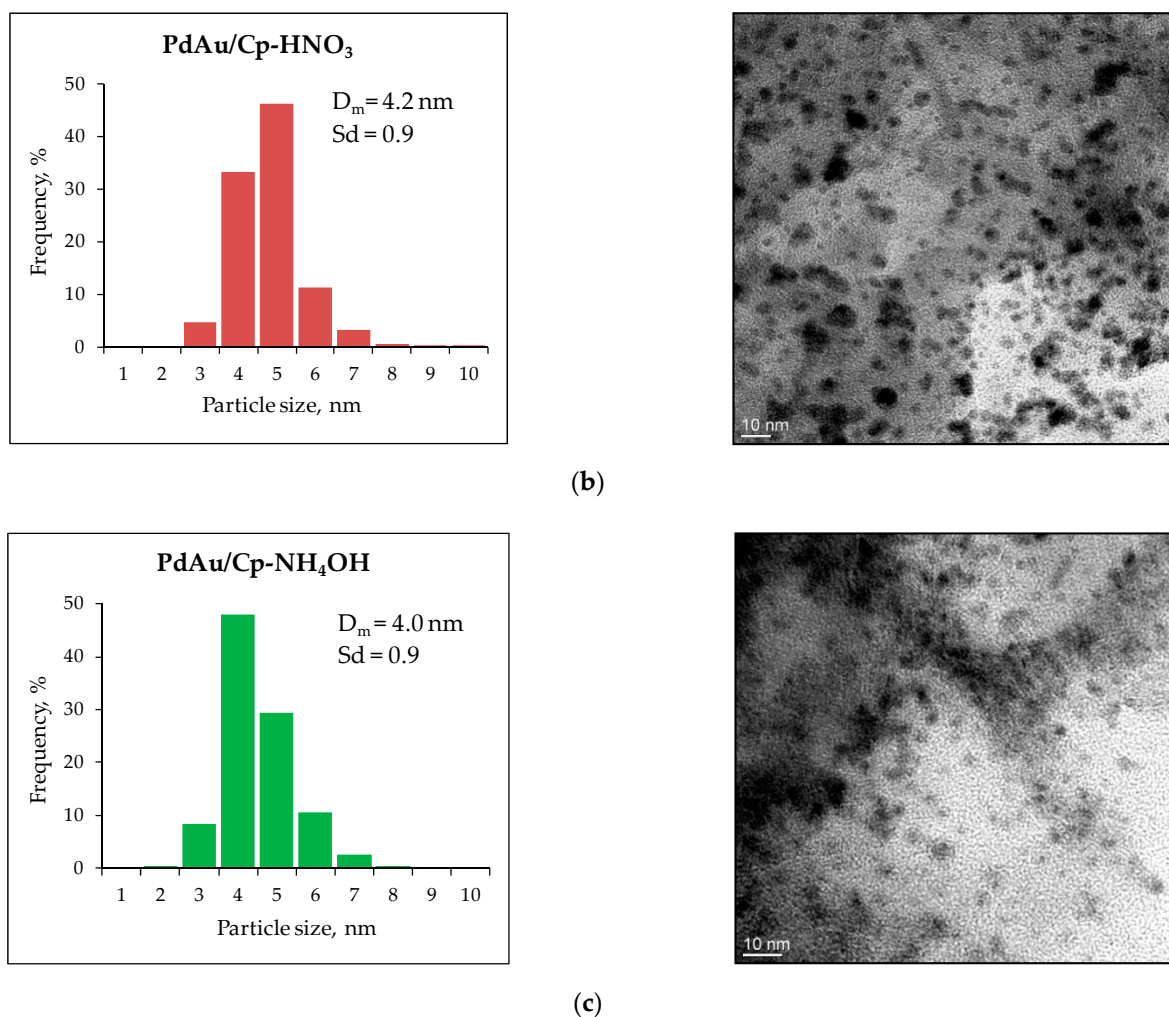


Figure 4. Metal particle size distribution and HRTEM images of PdAu/Cp (a), PdAu/Cp-HNO₃ (b) and PdAu/Cp-NH₄OH (c) catalysts.

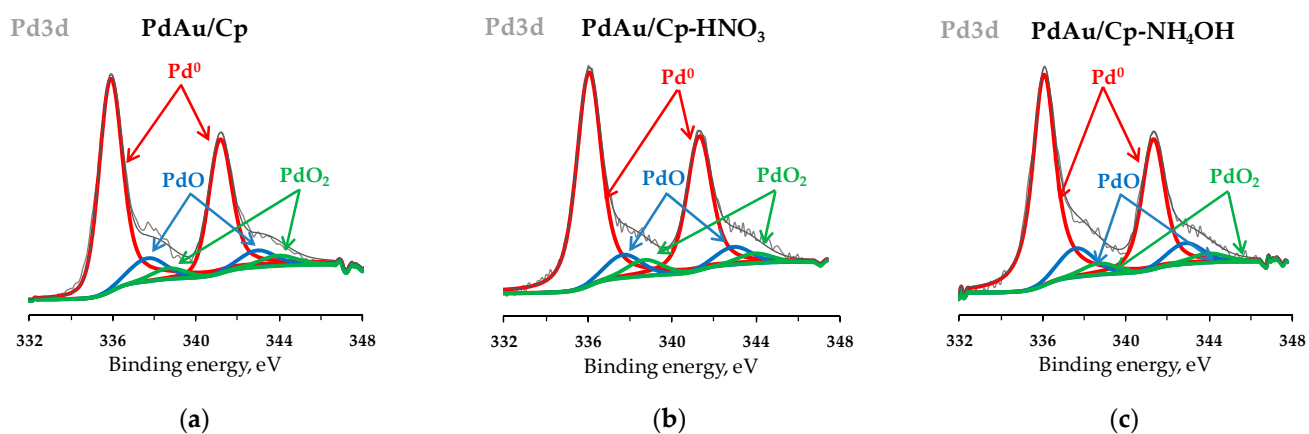


Figure 5. Cont.

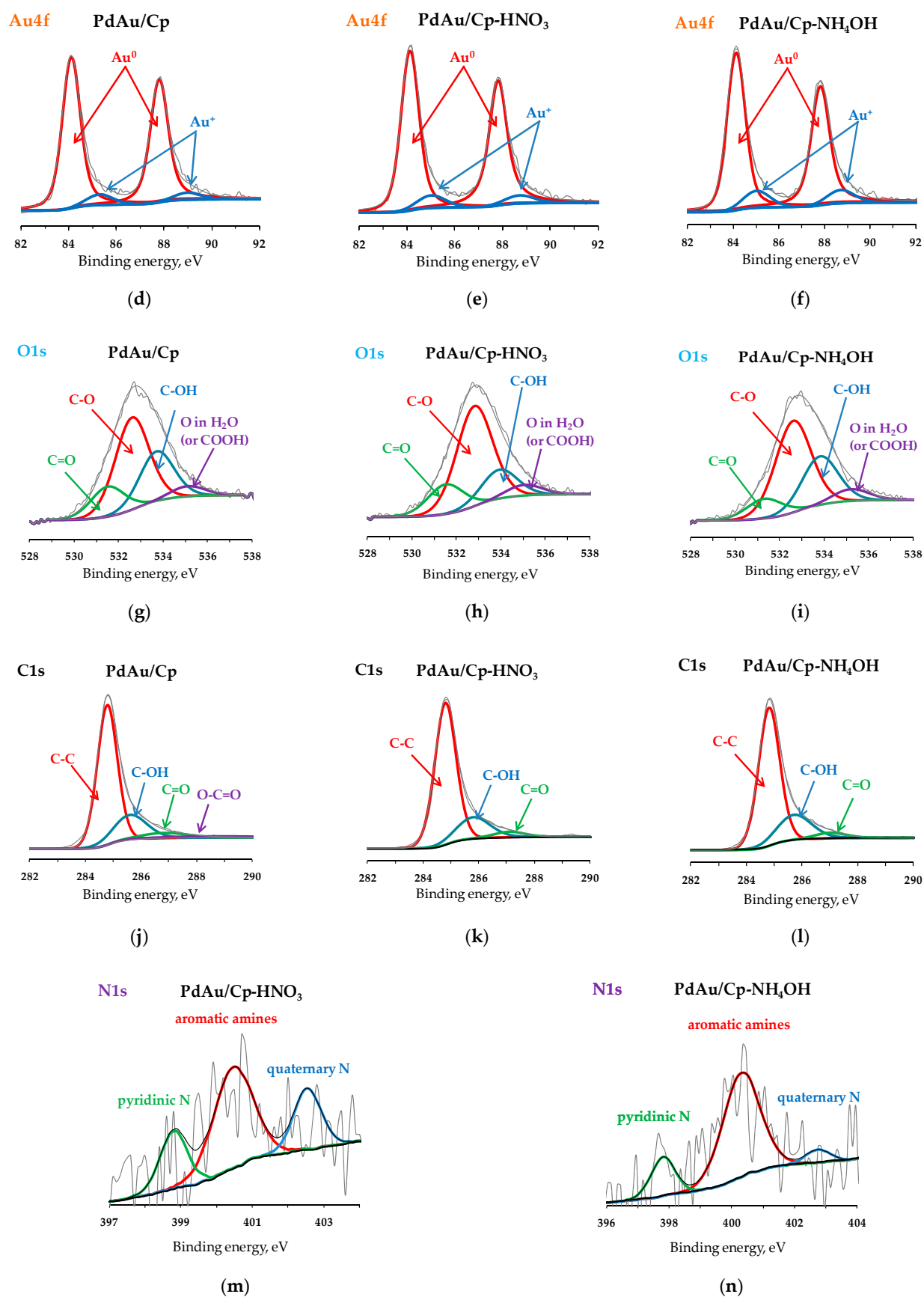


Figure 5. XPS spectra of Pd3d (a–c), Au4f (d–f), O1s (g–i), C1s (j–l), N1s (m,n) peaks for catalysts PdAu/Cp (a,d,i,j), PdAu/Cp-HNO₃ (b,e,h,k,m) and PdAu/Cp-NH₄OH (c,f,i,l,n), and assignments of their deconvoluted components.

Table 5. Effect of modification of the support on contribution of different electronic states of Pd and Au calculated according to XPS.

Catalyst	Pd ^(0, 2+ or 4+) Relative Content, %			Au ^(0 or 1+) Relative Content, %	
	Pd ⁰ (335.9–336.1 eV)	Pd ²⁺ (337.7–337.8 eV)	Pd ⁴⁺ (338.7 eV)	Au ⁰ (84.1–84.2 eV)	Au ¹⁺ (85.2–85.4 eV)
PdAu/Cp	84	9	7	93	7
PdAu/Cp-HNO ₃	83	10	7	91	9
PdAu/Cp-NH ₄ OH	83	12	5	88	12

Table 6. Elements surface concentration (at.%) determined by XPS.

Element	PdAu/Cp	PdAu/Cp-HNO ₃	PdAu/Cp-NH ₄ OH
C1s	95.3	94.3	94.3
N1s	0.06	0.14	0.26
O1s	2.9	4.0	3.9
Pd3d	1.3	1.2	1.2
Au4f	0.4	0.3	0.3

For all investigated catalysts, O1s peak can be decomposed into four peaks (Figure 5g–i): (i) BE 531.5–531.6 eV, associated with oxygen atoms that are part of carbonyl groups with (C=O); (ii) BE 532.5–532.7 eV, oxygen bonded to carbon atoms by a single bond with (C–O); (iii) BE 533.7–533.9 eV, in hydroxyl groups C–OH; and (iv) BE 535.0–535.1 eV in carboxyl groups and/or adsorbed water (O in H₂O or COOH) [46–48]. The relative contribution of each type of oxygen is presented in Table 7. The main contribution is from oxygen bonded to carbon atoms by a single bond (50–59%). The contribution of oxygen of the hydroxyl and carbonyl groups varies from 17 to 28% and 11 to 18%, respectively. The amount of oxygen in the form of adsorbed water and/or carboxyl groups was approximately the same for all studied samples. The modified support samples had a slightly increased content of the surface oxygen concentration (3.9–4%) compared to the O1s content (2.9 at.%) in PdAu/Cp (Table 6).

Table 7. Effect of modification of support on contribution of different electronic states of oxygen calculated according to XPS.

Catalyst	Oxygen Relative Content, at.%			
	C=O (531.5–531.6 eV)	C–O (532.5–532.7 eV)	C–OH (533.7–533.9 eV)	O in H ₂ O or COOH (535.0–535.1 eV)
PdAu/Cp	16	50	28	6
PdAu/Cp-HNO ₃	18	59	17	6
PdAu/Cp-NH ₄ OH	11	53	28	8

C1s spectrum (Figure 5j–l) can be deconvoluted into four components characterizing the state of carbon in: C–C (BE 284.8 eV), C–OH (BE 285.5–285.7 eV), C=O (BE 286.8–287.0 eV) and O–C=O, carboxyls, lactones and esters (BE 288.5–288.7 eV) [49–51]. The exception were the modified samples, where the O–C=O state of carbon is absent. Based on the analysis of the contribution of various states of carbon (Table 8), the following conclusions can be drawn: the main contribution is made by C–C, which relative content varies from 72 to 78%; the carbon content in the oxygen-containing functional groups is in the range of 18–22%. Summarizing, modification of the Sibunit surface or the introduction of gold along with palladium has little effect on the contribution of the different carbon states. Additionally, not many changes in carbon surface concentration were observed for the modified samples in comparison to PdAu/Cp, since only a 1.1% reduction in surface carbon was observed for both pretreated catalysts (Table 6).

Table 8. Effect of modification of support on contribution of different electronic states of carbon calculated according to XPS.

Catalyst	Carbon Relative Content, %			
	C–C (284.8 eV)	C–OH (285.5–285.7 eV)	C=O (286.8–287.0 eV)	O–C=O (288.5–288.7 eV)
PdAu/Cp	72	21	6	1
PdAu/Cp-HNO ₃	78	18	4	0
PdAu/Cp-NH ₄ OH	74	22	4	0

N1s spectrum was only analyzed for the modified Sibunit containing samples (Figure 5m,n). Low surface nitrogen concentration complicated this peak interpretation for the unmodified sample. At the same time, for PdAu/Cp-NH₄OH, nitrogen surface concentration was almost twofold higher than for PdAu/Cp-HNO₃ (Table 6). This shows incorporation of N into Sibunit supports during HNO₃ and NH₄OH treatment. Deconvolution of asymmetric N1s spectra identified that the incorporated N species were pyridinic (BE 397.8–398.4 eV), in aromatic amines –NH₂ aniline and/or imines C=NH (BE 400.5 eV) or quaternary nitrogen (BE 401–402.6 eV) [52–54]. The calculated proportions of each state displayed in Table 9 show that both samples have predominance of aromatic amines. However, PdAu/Cp-NH₄OH has higher relative contribution of aromatic nitrogen species, while PdAu/Cp-HNO₃ is characterized by higher quaternary nitrogen contribution.

Table 9. Effect of modification of support on contribution of different species of nitrogen calculated according to XPS.

Catalyst	Nitrogen Relative Content, %		
	Pyridinic N (397.8–398.8 eV)	Aromatic Amines (400.3–400.5 eV)	Quaternary N (401–402.6 eV)
PdAu/Cp-HNO ₃	22	55	23
PdAu/Cp-NH ₄ OH	18	76	6

In general, from the XPS results on element surface content (Table 6), it can be concluded that bimetallic catalysts on pretreated Sibunit supports are different from the untreated catalyst, by slightly increased oxygen content and the presence of nitrogen, with the latter higher for PdAu/Cp-NH₄OH. Surface concentration of Pd and Au was practically the same for all catalysts. Thus, the modification with nitric acid and ammonium hydroxide leads to the functionalization of the Sibunit surface with oxygen and nitrogen species, which can play an important role in modifying the carbon support properties. Such hetero-atoms can not only change the polarity and electronic properties of carbon materials, but also improve the reactivity of the catalysts [55–58].

Figure 6 and Table 10 show the distribution and concentration of acid-base sites on the surface of the supports and their corresponding catalysts, determined by the Hammett indicator method. The analysis of the results indicates the predominance of Brønsted acid and basic centers (BAC and BBC) on the surface of all studied samples. The concentration of Lewis acid and basic centers (LAC and LBC) did not change neither after the modification of Sibunit nor after the introduction of palladium and gold on all supports. The distribution of BAC and BBC also changed slightly when Sibunit was modified with NH₄OH and/or after the deposition of a bimetallic system on Cp and Cp-NH₄OH (Figure 6a,c). However, upon modification of Sibunit with HNO₃ (Figure 6b), the concentration of BAC and BBC decreased by almost one half in comparison with the unmodified support. On the contrary, after the deposition of Pd and Au on Cp-HNO₃, the number of these centers increased almost to the values found for PdAu/Cp and PdAu/Cp-NH₄OH.

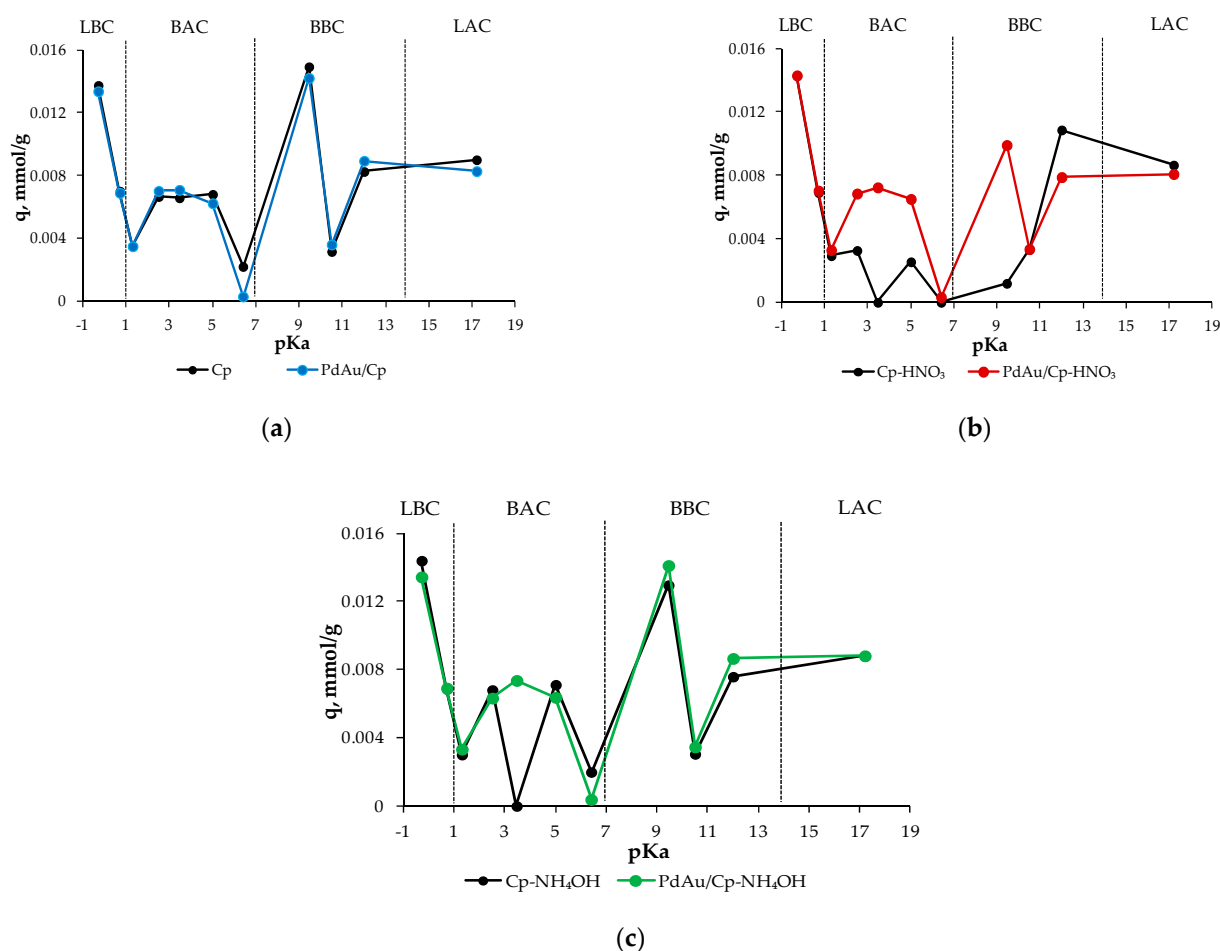


Figure 6. Distribution of acid-base adsorption centers on the surface of PdAu/Cp (a), PdAu/Cp-HNO₃ (b) and PdAu/Cp-NH₄OH (c) catalysts and their corresponding supports.

Thus, not many changes in acid-base properties were observed among the three bimetallic systems excepting the lower BBC concentration for PdAu/Cp-HNO₃. This correlates with the XPS data, where both carbon and oxygen atoms from hydroxyl groups (C-OH, Tables 7 and 8) were also in lower amounts in comparison to PdAu/Cp and PdAu/Cp-NH₄OH.

The obtained results of morphology, and the textural, structural, electronic and acid-base properties do not show much change for the studied bimetallic catalysts. However, if we compare the distinctive data on nitrogen content and relative contribution of divalent palladium and, notably, monovalent gold with selectivity to FDCA (Table 11), the following correlation can be observed: the higher the nitrogen content, the larger the contribution of Pd²⁺ and Au⁺, the active sites for the production of diacid according to some works [9,19,59–61]. Namely, Chen et al. [9] found a structure–activity correlation and demonstrated that the heteroatoms-doped supports enhance the fraction of surface Pd²⁺ species, which plays a crucial role in reducing of the activation energies of both HMF conversion and FDCA formation. At the same time, the positively charged Au nanoparticles attract OH[−] ions, which results in an increase in dehydrogenation activity (last step for FDCA formation) [19,59].

Thus, the most active catalyst has the largest contribution of Pd²⁺ and Au⁺ and, most importantly, an increased amount of nitrogen heteroatoms, comparable to the gold content in the samples (≈0.3 at.%). The presence of N on the carbon surface can influence the oxidation state of active sites (Pd²⁺ and Au⁺). In turn, nitrogen-containing groups promoted basic properties, which also could favor diacid formation. However, a deeper study of these and new nitrogen-doped Sibunit noble metal-based catalysts is required for understanding

the promoting effect of functionalization by nitrogen in detail. Moreover, analyzing the dependence of the catalytic activity on the average size of bimetallic nanoparticles, at first glance, there is no correlation between these parameters. At the same time, as shown in our previous work [24], the dependence of the catalytic activity, in particular TOF, on the average size of gold nanoparticles can be volcano type behavior, indicating the optimal size of gold nanoparticles required to achieve the highest TOF value. Analysis of the data allows suggesting that in the present study as in [62], a similar dependence of the catalytic activity on the average size of bimetallic nanoparticles can be observed. Thus, the oxidation of HMF to FDCA is a structure-sensitive reaction requiring an optimal bimetallic nanoparticle size of about 4 nm.

Table 10. The content of acid-base centers on the surface of the studied catalysts and corresponding supports (q, $\mu\text{mol/g}$).

Indicator	pKa	SAMPLE					
		Cp	PdAu/Cp	Cp-HNO ₃	PdAu/Cp-HNO ₃	Cp-NH ₄ OH	PdAu ₂ /Cp-NH ₄ OH
LEWIS BASE							
2-Nitroaniline	−0.29	13.7	13.4	14.3	14.3	14.4	13.5
BRØNSTED ACID							
2,4,6-Trinitrophenol	0.71	7.0	6.9	6.9	7.0	6.9	6.9
Brilliant green	1.30	3.5	3.5	2.9	3.3	3.0	3.3
3-Nitroaniline	2.50	6.7	7.0	3.3	6.9	6.8	6.3
Methyl orange	3.46	6.6	7.1	0	7.2	0	7.4
Methyl Red	5.00	6.8	6.2	2.6	6.5	7.1	6.4
Bromocresol purple	6.40	2.2	0.3	0	0.3	2.0	0.4
Σ		32.8	31.0	16.7	31.2	25.8	30.7
BRØNSTED BASE							
Catechol	9.45	14.9	14.2	1.2	9.9	13.0	14.1
Nile blue	10.50	3.2	3.6	3.3	3.4	3.1	3.5
Tropaeolin OO	12.00	8.3	8.9	10.9	7.9	7.6	8.7
Σ		26.4	26.7	15.4	21.2	23.7	26.3
LEWIS ACID							
2,4-Dinitrotoluene	17.20	9.0	8.3	8.7	8.1	8.8	8.8
TOTAL							
Σ		81.9	79.4	55.1	74.8	72.7	79.3

Table 11. Relation between structural and electronic properties of catalysts and their catalytic results.

Entry	Catalyst	N Content, at. %	Relative Content, %		FDCA Yield after 2h, %
			Pd ²⁺	Au ⁺	
1	PdAu/Cp	0.06	9	7	59
2	PdAu/Cp-HNO ₃	0.14	10	9	62
3	PdAu/Cp-NH ₄ OH	0.26	12	12	67

Separately, it should be noted that the possible reasons for the observed deactivation for PdAu/Cp-HNO₃ (Figure 1) is the agglomeration of nanoparticles, as well as the reduction of gold and palladium ions. Namely, acid pretreatment adversely affects the stabilization of Pd and Au NPs, which ultimately leads to a partial loss of activity. The same effect was observed by Donoeva et al. [59]: the maximum agglomeration of gold particles (from 4.3 to 10.3 nm) was found for Au deposited on high surface area graphite treated with HNO₃ vapor (Au/HSAG-ox) after 10 h of HMF oxidation reaction, while the

sample pretreated with gaseous NH_3 at 600 °C (Au/HSAG-N) showed the least particle growth (from 3.2 to 5.9 nm). At the same time, reduction of Au^+ and Pd^{2+} to metallic state could be the reason of the observed loss of activity due to the fact that the reverse transition of the metal to the ionic state is impossible for large nanoparticles.

3. Materials and Methods

Commercial $\text{Al}_2\text{O}_3\text{-V}$ (Versal gamma alumina (VGL-25), UOP, Des Plaines, IL, USA), AlOOH-C (boehmite (Catapal B), Sasol, Hamburg, Germany), AlOOH-S (silica-alumina hydrate (Siral 5), Sasol, Hamburg, Germany), carbon material Sibunit (Center of New Chemical Technologies of Boreskov Institute of Catalysis, Omsk, Russia) and TiO_2 (Titania P25 Evonik, Degussa GmbH, Essen, Germany) were used as supports.

Titania was modified by impregnation ($2.5 \text{ cm}^3/\text{g}$) with aqueous solutions of precursors $\text{Fe}(\text{NO}_3)_3 \cdot 9\text{H}_2\text{O}$, $\text{Ce}(\text{NO}_3)_3 \cdot 6\text{H}_2\text{O}$, $\text{Mg}(\text{NO}_3)_2 \cdot 6\text{H}_2\text{O}$ and $\text{La}(\text{NO}_3)_3 \cdot 6\text{H}_2\text{O}$ (Sigma-Aldrich, St. Louis, MO, USA). The impregnated supports were dried at room temperature for 48 h, then at 110 °C for 4 h and finally dried at 550 °C in static air for 4 h. Modified titania was denoted as $\text{M}_x\text{O}_y/\text{TiO}_2$ (where $\text{M}_x\text{O}_y = \text{CeO}_2, \text{La}_2\text{O}_3, \text{Fe}_2\text{O}_3$ or MgO).

Modification of Sibunit carbon (hereafter denoted as Cp) with HNO_3 or NH_4OH (denoted as Cp- HNO_3 or Cp- NH_4OH , respectively) was as follows: Sibunit was boiled with a 20 wt.% solution of nitric acid or ammonium hydroxide, respectively, for 1 h, then washed with distilled water and dried at 80 °C for 2 h.

Au was loaded (nominal loading 4 wt.%) on $\text{M}_x\text{O}_y/\text{TiO}_2$ and various alumina supports using $\text{HAuCl}_4 \cdot 3\text{H}_2\text{O}$ (Merck, Darmstadt, Germany) as precursor, by the deposition-precipitation method with urea (Merck, Darmstadt, Germany) in the absence of light, according to the procedure described in previous works [20–24]. Gold catalyst samples (0.5 g) were then pretreated in a hydrogen atmosphere for 1 h at 300 °C (15% H_2 in Ar, 300 mL/min flow rate) for the decomposition of the hydrolysis products of the complex of gold (III) with urea on the support surface [63].

Ag/ $\text{CeO}_2/\text{TiO}_2$ catalyst (2.3 wt.% Ag nominal loading) was prepared by deposition-precipitation with NaOH using AgNO_3 (Sigma-Aldrich, St. Louis, MO, USA) as a precursor in the absence of light, following the previously reported procedure [25].

Pd/ AlOOH-S catalyst (1.0 wt.% Pd nominal loading) was prepared by the deposition-precipitation method with NaOH described in [64]. A weighed portion of PdCl_2 ($1.9 \times 10^{-3} \text{ M}$) was dissolved in water with an excess of HCl (pH = 2), followed by support addition. Then the pH was adjusted to 10, which was reached with a 0.1 M NaOH solution. The synthesis was carried out for 3 h at room temperature under vigorous stirring. The catalyst was then centrifuged and washed with distilled water seven times until complete chloride removal, which was checked by using the silver nitrate test. The resulting catalyst was dried under vacuum at 80 °C for 4 h, and then reduced at 300 °C under a flow of 15% H_2 in Ar for 1 h (flow rate = 300 mL/min, 0.5 g catalyst).

Pd/Cp, Au/Cp and Ag/Cp catalysts (1 wt.% of noble metal) were synthesized by the sol immobilization method [65]. Briefly, 1 mL of a solution of AgNO_3 , $\text{NaAuCl}_4 \cdot \text{H}_2\text{O}$ or Na_2PdCl_4 (Merck, Darmstadt, Germany), (10 mg Ag or Pd/mL H_2O , 5 mg Au/mL H_2O) and 0.5 mL of polyvinyl alcohol (PVA) solution (1% w/w, Merck, Darmstadt, Germany) were added to 100 mL of Milli-Q water. After 5 min of vigorous stirring, a solution of NaBH_4 (Merck, Darmstadt, Germany) ($\text{Me}/\text{NaBH}_4 = 1/4 \text{ mol/mol}$) was added to form a brown sol. After 30 min, the support was added (in the amount necessary to obtain 1 wt.% Me catalyst) with a few drops of H_2SO_4 (Merck, Darmstadt, Germany) to immobilize metal nanoparticles on the support. The deposition was carried out for 1 h, and the resulting catalyst was then washed and dried at 80 °C for 2 h in air.

PdAu/Cp, PdAu/Cp- HNO_3 , PdAu/Cp- NH_4OH were synthesized also by the sol immobilization method (assuming that the catalyst would contain 1 wt.% metals with a Pd:Au ratio of 4:1 mol/mol), described above [65].

Palladium and gold contents were measured by inductively coupled plasma atomic emission spectroscopy (ICP-AES) in an iCAP 6300 Duo spectrometer (Thermo Fisher

Scientific, Waltham, MA, USA) and X-ray energy dispersive spectroscopy (XEDS) in a JEOL JEM-2100F electronic microscope (JEOL Ltd., Tokyo, Japan) equipped with an Oxford INCA X-sight system detector (Oxford Instruments, Abingdon, Oxfordshire, UK).

XRD patterns were recorded using a Bruker D8 X-ray diffractometer (Bruker Corporation, Billerica, MA, USA) and CuK α as X-ray source ($\lambda = 0.15406$ nm) with a scanning range of $2\theta = 10\text{--}90^\circ$.

Textural properties were studied using an ASAP 2060 (Micromeritics Instrument Corporation, Norcross, GA, USA) apparatus. Catalysts were previously degassed in vacuum at 300°C for 5 h. The surface area and pore size distribution were calculated using the Brunauer-Emmett-Teller (BET) equation applied for the adsorption isotherm at the relative pressures between 0.005 to 0.25 and Barrett-Joyner-Halenda (BJH) method (desorption branch), respectively.

Size distribution of Pd-Au particles was studied by high resolution transmission electron microscopy (HRTEM) using a JEOL JEM-2100F (JEOL Ltd., Tokyo, Japan) with a sample preparation system. The samples were dispersed to a fine powder and sonicated in hexane at room temperature. Derived suspension was applied on a carbon-coated Cu grid. For each sample, at least 700 particles were counted.

Surface composition and the chemical state of Pd, Au, O, N and C were determined by X-ray photoelectron spectroscopy (XPS) analysis, performed on an ESCALAB 200A spectrometer (VG Scientific, Waltham, MA, USA) using Al K α radiation (1486.6 eV). A pass-energy of 40 eV and a step size of 0.1 eV were selected. The charge effect was corrected using the C1s peak as a reference (binding energy of 285 eV). The CASA XPS software (version 2.3.15, CASA Software Ltd., Teignmouth, UK, <http://www.casaxps.com/>) was used for data analysis.

Acid-base properties of supports and catalysts were studied by the Hammett indicator method using 11 indicators with pK_a values in the range from -0.29 to 17.2 . For this purpose, the optical density of the initial solutions of indicators (D_0) was measured on a Cary 60 UV spectrophotometer (Agilent Technologies, Santa Clara, CA, USA). Then, suspensions of supports and catalysts were prepared in these solutions, and after the establishment of adsorption equilibrium and subsequent centrifugation and decantation, the optical density D_1 was determined. To take into account the effect of the change in the pH of the medium and the dissolution of the sample on the optical density upon contact of the material with the solution, a suspension of the sorbent in distilled water was obtained. After 2 h, an indicator solution was added to the decantate and the optical density (D_2) was measured. All determinations were carried out in cuvettes at a wavelength that corresponds to the maximum absorption of the indicator solution.

The content of active sites (q_{pKa} , $\mu\text{mol/g}$) with a given pK_a value was calculated using Equation (1):

$$q_{\text{pKa}} = \frac{C_{\text{ind}} \cdot V_{\text{ind}}}{D_0} \cdot \left[\frac{|D_0 - D_1|}{\alpha_1} \right] \pm \left[\frac{|D_0 - D_2|}{\alpha_2} \right] \quad (1)$$

where C_{ind} and V_{ind} are the concentration and volume of the indicator, α_1 and α_2 are the mass of the sample when measuring D_1 and D_2 . The “−” sign corresponds to the unidirectional change of D_1 and D_2 relative to D_0 . The “+” sign is for multidirectional [66].

Catalytic tests were carried out at 60°C under 3 atm of oxygen in a semi-batch reactor with stirring at 1100 rpm. Typically, the catalyst sample was added in a HMF/Me (Me = Ag, Au, Pd, PdAu) ratio $R = 200$ mol/mol to 150 mL of 0.15 M HMF or Catalyst: HMF = (0.19–0.49):1 (*wt/wt*) and 0.3 M NaOH aqueous solution (distilled water), in a glass reactor equipped with heater, mechanical stirrer, gas supply system and thermometer. Small aliquots of the reacting mixture were taken after 15, 30, 60, 120, and in some cases, 180, 240 and 360 min, for monitoring the reaction progress. HMF and NaOH (Merck, Darmstadt, Germany) were used as reagents.

Reactants and products were periodically analyzed and quantified by high-performance liquid chromatography (HPLC, Agilent Technologies, 1220 Infinity, Santa Clara, CA, USA) using a column Alltech OA-10308 ($L \times \text{i.d.}: 300 \text{ mm} \times 7.8 \text{ mm}$, Fisher Scientific, Hampton,

NH, USA) with ultraviolet (Varian 9050 UV, 210 nm, Varian Inc, Palo Alto, CA, USA) and refractive index (Waters RI, Waters Co, Milford, MA, USA) detectors. 0.4 mL/min of 0.1% aqueous solution of H₃PO₄ used as the eluent. The identification of compounds was achieved by calibration using reference commercial samples. The difference in concentration from the carbon mass balance was attributed to unknown products detected on HPLC chromatograms.

Conversion of HMF, selectivity and yield to products (5-hydroxymethyl-2-furancarboxylic acid (HFCA) and FDCA) and carbon balance, were calculated according to Equations (2)–(5), respectively:

$$\text{Conversion (\% mol)} = \frac{\text{C moles of all products}}{\text{C moles of HMF}} \times 100 \quad (2)$$

$$\text{Selectivity of product } i \text{ (\% mol)} = \frac{\text{C moles of product } i \text{ formed}}{\text{C moles of all products}} \times 100 \quad (3)$$

$$\text{Yield of product } i \text{ (\% mol)} = \frac{\text{C moles of product } i \text{ formed} \times \text{C balance}}{\text{Initial C moles of HMF}} \quad (4)$$

$$\text{C balance (\% mol)} = 100 - \frac{\text{Initial C moles of HMF} - \text{Final C of all products}}{\text{Initial C moles of HMF}} \times 100 \quad (5)$$

The carbon balance obtained in each catalytic reaction was always in the 95–100% range, with the exception of silver catalysts.

4. Conclusions

The efficiency of Ag, Au, Pd and bimetallic PdAu NPs supported on different materials (unmodified and modified titania, commercial alumina and untreated and treated Sibunit carbon support) was investigated for aerobic oxidation of 5-hydroxymethyl-2-furfural into high valuable 2,5-furandicarboxylic (FDCA) under mild conditions ($T = 60^\circ\text{C}$, 3 atm of O₂, water as solvent and 2 equiv. NaOH).

The highest FDCA selectivity was obtained when the active metals were supported on Sibunit, while the order of catalyst selectivity in terms of noble metal was as follows: Ag < Au < Pd < PdAu. The low activity of silver is due to that it cannot suppress HMF degradation to polymeric products (humins) occurring under basic conditions.

The positive effect of the treatment of Sibunit with HNO₃ or NH₄OH for FDCA production with bimetallic PdAu nanoparticles was revealed. Thus, the highest FDCA yield in this work (76 mol.%) was obtained on PdAu/Cp-NH₄OH after 6 h.

The FDCA selectivity seems to be affected by the amount of nitrogen on carbon support surface, found after both treatments. The highest nitrogen content was detected on PdAu/Cp-NH₄OH. These hetero-atoms can possibly influence the oxidation state of the active metals (Pd²⁺ and Au⁺), which are suggested to be the active sites for FDCA formation. Additionally, it was revealed that the oxidation of HMF towards FDCA is a structure-sensitive reaction, requiring an optimal PdAu NPs size of about 4 nm, obtained for PdAu/Cp-NH₄OH.

Supplementary Materials: The following are available online at <https://www.mdpi.com/2073-4344/11/1/115/s1>, Figure S1: N₂ isotherms for Cp (a), and PdAu/Cp (b), Cp-HNO₃ (c), and PdAu/Cp-HNO₃ (d), Cp-NH₄OH (e) and PdAu/Cp-NH₄OH (f).

Author Contributions: D.G. was responsible for preparation of supported Ag, Au, Pd, Pd-Au on Sibunit and Au/Alumina, performed catalytic tests on these materials and Hammett indicator method, interpreted XPS, XRD and TEM results and contributed to the writing; E.P. carried out catalysts preparation of Au/Me_xO_y/TiO₂, performed preliminary catalytic tests on these materials, and wrote the first draft of the paper; E.K. was responsible for methodology of catalytic tests with supported Ag, Au, Pd, Pd-Au on Sibunit materials and Au/Alumina, supervised those experiments, participated on the conceptualization and methodology of most characterization methods and contributed to the writing; S.A.C.C. was responsible for the XPS and BET analyses; M.S., A.V. and L.P.

dealt with methodology of preliminary catalytic tests; M.S., A.V., L.P., S.A.C.C., N.B., V.C.C. and A.P. provided the means for the realization of this work and contributed to the supervision and paper revision. All authors have read and agreed to the published version of the manuscript.

Funding: This work was partially supported by Fundação para a Ciência e Tecnologia (FCT), Portugal, through project UIDB/00100/2020 of the Centro de Química Estrutural, Associate Laboratory for Green Chemistry—LAQV, financed by national funds from FCT/MCTES (UIDB/50006/2020), FCT Scientific Employment Stimulus- Institutional Call (CEECINST/00102/2018) and PTDC/QEQ-QIN/3967/2014, Tomsk Polytechnic University Competitiveness Enhancement Program project VIU-RSCBMT-197/2020, Russian Foundation of Basic Research, project 18-29-24037, Tomsk Polytechnic University State Task ‘Science’ (project FSWW-2020-0011) and MICINN project CTQ2017-86170-R (Spain).

Institutional Review Board Statement: Not applicable.

Informed Consent Statement: Not applicable.

Data Availability Statement: Data available upon request.

Acknowledgments: TEM and EDX analysis was carried out at the Innovation Centre for Nanomaterials and Nanotechnologies of Tomsk Polytechnic University. ICP-AES performed using the core facilities of TPU’s “Physics and Chemical methods of analysis”. Authors thank Carlos Sá (CEMUP) for the assistance with XPS analyses. We also thank the colleagues from the Center of New Chemical Technologies of Boreskov Institute of Catalysis, Omsk, Russia, for providing samples of the Sibunit carbon support.

Conflicts of Interest: The authors declare no conflict of interest.

References

1. Li, H.; Bhadury, P.S.; Riisager, A.; Yang, S. One-pot transformation of polysaccharides via multi-catalytic processes. *Catal. Sci. Technol.* **2014**, *4*, 4138–4168. [\[CrossRef\]](#)
2. Climent, M.J.; Corma, A.; Iborra, S. Conversion of biomass platform molecules into fuel additives and liquid hydrocarbon fuels. *Green Chem.* **2014**, *16*, 516–547. [\[CrossRef\]](#)
3. Roman-Leshkov, Y.; Barret, C.J.; Liu, Z.Y.; Dumesic, J.A. Production of dimethylfuran for liquid fuels from biomass-derived carbohydrates. *Nature* **2007**, *447*, 982–985. [\[CrossRef\]](#) [\[PubMed\]](#)
4. Corma, A.; Iborra, S.; Velty, A. Chemical Routes for the Transformation of Biomass into Chemicals. *Chem. Rev.* **2007**, *107*, 2411–2502. [\[CrossRef\]](#)
5. Bozell, J.J.; Petersen, G.R. Technology development for the production of biobased products from biorefinery carbohydrates—the US Department of Energy’s “Top 10” revisited. *Green Chem.* **2010**, *12*, 539–554. [\[CrossRef\]](#)
6. Van Putten, R.-J.; Van der Waal, J.C.; De Jong, E.; Rasrendra, C.B.; Heeres, H.J.; De Vries, J.G. Hydroxymethylfurfural, A Versatile Platform Chemical Made from Renewable Resources. *Chem. Rev.* **2013**, *113*, 1499–1597. [\[CrossRef\]](#)
7. Toshinari, M.; Hirokazu, K.; Takenobu, K.; Hirohide, M. Method for Producing Furan-2,5-Dicarboxylic Acid. U.S. Patent No. 2007/0232815A1, 4 October 2007.
8. Miura, T.; Kakinuma, H.; Kawano, T.; Matshisa, H. Method for Producing Furan-2,5-Dicarboxylic Acid. U.S. Patent No. 7411078B2, 12 August 2008.
9. Chen, C.; Li, X.; Wang, L.; Liang, T.; Wang, L.; Zhang, Y.; Zhang, J. Highly Porous Nitrogen and Phosphorus-Codoped Graphene: An Outstanding Support for Pd Catalysts to Oxidize 5-Hydroxymethylfurfural into 2,5-Furandicarboxylic Acid. *ACS Sustain. Chem. Eng.* **2017**, *5*, 1300–11306. [\[CrossRef\]](#)
10. Siyo, B.; Schneider, M.; Radnik, J.; Pohl, M.-M.; Langer, P.; Steinfeldt, N. Influence of support on the aerobic oxidation of HMF into FDCA over preformed Pd nanoparticle based materials. *Appl. Catal. A* **2014**, *478*, 107–116. [\[CrossRef\]](#)
11. Zheng, L.; Zhao, J.; Du, Z.; Zong, B.; Liu, H. Efficient aerobic oxidation of 5-hydroxymethylfurfural to 2,5-furandicarboxylic acid on Ru/C catalysts. *Sci. China Chem.* **2017**, *60*, 950–957. [\[CrossRef\]](#)
12. Megías-Sayago, C.; Lolli, A.; Ivanova, S.; Albonetti, S.; Cavani, F.; Odriozola, J.A. Au/Al₂O₃—Efficient catalyst for 5-hydroxymethylfurfural oxidation to 2,5-furandicarboxylic acid. *Catal. Today* **2019**, *333*, 169–175. [\[CrossRef\]](#)
13. Schade, O.R.; Kalz, K.F.; Neukum, D.; Kleist, W.; Grunwaldt, J.-D. Supported gold- and silver-based catalysts for the selective aerobic oxidation of 5-(hydroxymethyl)furfural to 2,5-furandicarboxylic acid and 5-hydroxymethyl-2-furancarboxylic acid. *Green Chem.* **2018**, *20*, 3530–3541. [\[CrossRef\]](#)
14. Davis, S.E.; Houk, L.R.; Tamargo, E.C.; Datye, A.K.; Davis, R.J. Oxidation of 5-hydroxymethylfurfural over supported Pt, Pd and Au catalysts. *Catal. Today* **2011**, *160*, 55–60. [\[CrossRef\]](#)
15. Lolli, A.; Albonetti, S.; Utili, L.; Amadori, R.; Ospitali, F.; Lucarelli, C.; Cavani, F. Insights into the reaction mechanism for 5-hydroxymethylfurfural oxidation to FDCA on bimetallic Pd–Au nanoparticles. *Appl. Catal. A* **2015**, *504*, 408–419. [\[CrossRef\]](#)

16. Wang, Q.; Hou, W.; Li, S.; Xie, J.; Li, J.; Zhou, Y.; Wang, J. Hydrophilic mesoporous poly(ionic liquid)-supported Au–Pd alloy nanoparticles towards aerobic oxidation of 5-hydroxymethylfurfural to 2,5-furandicarboxylic acid under mild conditions. *Green Chem.* **2017**, *19*, 3820–3830. [[CrossRef](#)]
17. Villa, A.; Schiavoni, M.; Campisi, S.; Veith, G.M.; Prati, L. Pd-modified Au on carbon as an effective and durable catalyst for the direct oxidation of HMF to 2,5-furandicarboxylic acid. *ChemSusChem* **2013**, *6*, 609–612. [[CrossRef](#)] [[PubMed](#)]
18. Campisi, S.; Capelli, S.; Motta, D.; Trujillo, F.J.S.; Davies, T.E.; Prati, L.; Dimitratos, N.; Villa, A. Catalytic Performances of Au–Pt Nanoparticles on Phosphorous Functionalized Carbon Nanofibers towards HMF Oxidation. *Carbon* **2018**, *4*, 48. [[CrossRef](#)]
19. Zope, B.N.; Hibbitts, D.D.; Neurock, M.; Davis, R.J. Reactivity of the Gold/Water Interface During Selective Oxidation Catalysis. *Science* **2010**, *330*, 74–78. [[CrossRef](#)]
20. Pakrieva, E.; Kolobova, E.; Mamontov, G.; Bogdanchikova, N.; Farias, M.H.; Pascual, L.; Cortés Corberán, V.; Martínez Gonzalez, S.; Carabineiro, S.A.C.; Pestryakov, A. Green oxidation of n-octanol on supported nanogold catalysts: Formation of gold active sites under combined effect of gold content, additive nature and redox pretreatment. *ChemCatChem* **2019**, *11*, 1615–1624. [[CrossRef](#)]
21. Pakrieva, E.; Kolobova, E.; Kotolevich, Y.; Pascual, L.; Carabineiro, S.A.C.; Kharlanov, A.N.; Pichugina, D.; Nikitina, N.; German, D.; Zepeda Partida, T.A.; et al. Effect of gold electronic state on the catalytic performance of nano gold catalysts in n-octanol oxidation. *Nanomaterials* **2020**, *10*, 880. [[CrossRef](#)]
22. Pakrieva, E.; Kolobova, E.; German, D.; Stucchi, M.; Villa, A.; Prati, L.; Carabineiro, S.A.; Bogdanchikova, N.; Cortés Corberán, V.; Pestryakov, A. Glycerol Oxidation over Supported Gold Catalysts: The Combined Effect of Au Particle Size and Basicity of Support. *Processes* **2020**, *8*, 1016. [[CrossRef](#)]
23. Kolobova, E.N.; Pakrieva, E.G.; Carabineiro, S.; Bogdanchikova, N.; Kharlanov, A.; Kazantsev, S.O.; Hemming, J.; Mäki-Arvela, P.; Pestryakov, A.N.; Murzin, D. Oxidation of a wood extractive betulin to biologically active oxo-derivatives using supported gold catalysts. *Green Chem.* **2019**, *21*, 3370–3382. [[CrossRef](#)]
24. Kolobova, E.; Mäki-Arvela, P.; Grigoreva, A.; Pakrieva, E.; Carabineiro, S.A.C.; Peltonen, J.; Kazantsev, S.; Bogdanchikova, N.; Pestryakov, A.; Murzin, D.Y. Catalytic oxidative transformation of betulin to its valuable oxo-derivatives over gold supported catalysts: Effect of support nature. *Catal. Today* **2020**. [[CrossRef](#)]
25. Kolobova, E.; Kotolevich, Y.; Pakrieva, E.; Mamontov, G.; Farias, M.H.; Cortés Corberán, V.; Bogdanchikova, N.; Hemming, J.; Smeds, A.; Mäki-Arvela, P.; et al. Modified Ag/TiO₂ systems: Promising catalysts for liquid-phase oxidation of alcohols. *Fuel* **2018**, *234*, 110–119. [[CrossRef](#)]
26. Albonetti, S.; Lolli, A.; Morandi, V.; Migliori, A.; Lucarelli, C.; Cavani, F. On the mechanism of selective oxidation of 5-hydroxymethylfurfural to 2,5-furandicarboxylic acid over supported Pt and Au catalysts. *Appl. Catal. B Environ.* **2015**, *163*, 520–530. [[CrossRef](#)]
27. Chen, C.; Wang, L.; Zhu, B.; Zhou, Z.; El-Hout, S.I.; Yang, J.; Zhang, J. 2,5-Furandicarboxylic acid production via catalytic oxidation of 5-hydroxymethylfurfural: Catalysts, processes and reaction mechanism. *J. Energy Chem.* **2021**, *54*, 528–554. [[CrossRef](#)]
28. Rodríguez-Reinoso, F.; Sepúlveda-Escribano, A. Carbon as Catalyst support. In *Carbon Materials for Catalysis*; Serp, P., Figueiredo, J.L., Eds.; John Wiley & Sons: New York, NY, USA, 2009; pp. 131–155.
29. Auer, E.; Freund, A.; Pietsch, J.; Tacke, T. Carbons as supports for industrial precious metal catalysts. *Appl. Catal. A* **1998**, *173*, 259–271. [[CrossRef](#)]
30. Van Santen, R.A.; Van Leeuwen, P.W.N.M.; Moulijn, J.A.; Averill, B.A. Chapter 9: Preparation of catalyst supports, zeolites and mesoporous materials. Chapter 10: Preparation of Supported Catalysts. In *Studies in Surface Science and Catalysis*; Elsevier: Amsterdam, The Netherlands, 1999; Volume 123, pp. 433–485.
31. Surovikin, V.F.; Surovikin, Y.V.; Tsekhanovich, M.S. New fields in the technology for manufacturing carbon-carbon materials. Application of carbon-carbon materials. *Russ. J. Gen. Chem.* **2007**, *77*, 2301–2310. [[CrossRef](#)]
32. Dobrynkin, N.M.; Batygina, M.V.; Noskov, A.S.; Tsyrlunikov, P.G.; Shlyapin, D.A.; Schegolev, V.V.; Astrova, D.A.; Laskin, B.M. Catalysts Ru CeO₂/Sibunit for catalytic wet air oxidation of aniline and phenol. *Top. Catal.* **2005**, *33*, 69–76. [[CrossRef](#)]
33. Madsen, A.T.; RozmysBowicz, B.; Mäki-Arvela, P.; Simakova, I.L.; Eränen, K.; Murzin, D.Y.; Fehrmann, R. Deactivation in Continuous Deoxygenation of C18-Fatty Feedstock over Pd/Sibunit. *Top. Catal.* **2013**, *56*, 714–724. [[CrossRef](#)]
34. Zhang, Z.H.; Deng, K.J. Recent Advances in the Catalytic Synthesis of 2,5-Furandicarboxylic Acid and Its Derivatives. *ACS Catal.* **2015**, *5*, 6529–6544. [[CrossRef](#)]
35. Gorbanev, Y.Y.; Klitgaard, S.K.; Woodley, J.M.; Christensen, C.H.; Riisager, A. Gold-Catalyzed Aerobic Oxidation of 5-Hydroxymethylfurfural in Water at Ambient Temperature. *ChemSusChem* **2009**, *2*, 672–675. [[CrossRef](#)] [[PubMed](#)]
36. Taran, O.P.; Descorme, C.; Polyanskaya, E.M.; Ayusheyev, A.B.; Besson, M.; Parmon, V.N. Catalysts based on carbon material «Sibunit» for the deep oxidation of organic toxicants in water solutions. Aerobic oxidation of phenol in the presence of oxidized carbon and Ru/C catalysts. *Katal. Promyshlennosti* **2013**, *1*, 40–50. (In Russian)
37. Selen, V.; Güler, Ö.; Özer, D.; Evin, E. Synthesized multi-walled carbon nanotubes as a potential adsorbent for the removal of methylene blue dye: Kinetics, isotherms, and thermodynamics. *Desalination Water Treat.* **2015**, *57*, 1–13. [[CrossRef](#)]
38. Moulder, J.F.; Stickle, W.F.; Sobol, P.E.; Bomben, K.D. *Handbook of X-ray Photoelectron Spectroscopy*; Chastain, J., Ed.; Perkin-Elmer Corporation: Eden Prairie, MN, USA, 1992.
39. Boronin, A.I.; Slavinskaya, E.M.; Danilova, I.G.; Gulyaev, R.V.; Amosov, Y.; Kuznetsov, P.A.; Polukhina, I.A.; Koscheev, S.V.; Zaikovskii, V.I.; Noskov, A.S. Investigation of palladium interaction with cerium oxide and its state in catalysts for low-temperature CO oxidation. *Catal. Today* **2009**, *144*, 201–211. [[CrossRef](#)]

40. Mirkelamoglu, B.; Karakas, G. The role of alkali-metal promotion on CO oxidation over PdO/SnO₂ catalysts. *Appl. Catal. A Gen.* **2006**, *299*, 84–94. [[CrossRef](#)]
41. Mucalo, M.R.; Cooney, R.P.; Metson, J.B. Platinum and palladium hydrosols: Characterisation by X-ray photoelectron spectroscopy and transmission electron microscopy. *Colloids Surf.* **1991**, *60*, 175–197. [[CrossRef](#)]
42. Kibis, L.S.; Titkov, A.I.; Stadnichenko, A.I.; Koscheev, S.V.; Boronin, A.I. X-ray photoelectron spectroscopy study of Pd oxidation by RF discharge in oxygen. *Appl. Surf. Sci.* **2009**, *255*, 9248–9254. [[CrossRef](#)]
43. Díez, N.; Moysowicz, A.; Grylegicz, S.; Grzyb, B.; Gryglewicz, G. Enhanced reduction of graphene oxide by high-pressure hydrothermal treatment. *RSC Adv.* **2015**, *5*, 81831–81837. [[CrossRef](#)]
44. Ivanova, A.S.; Korneeva, E.V.; Slavinskaya, E.M.; Zyuzin, D.A.; Moroz, E.M.; Danilova, I.G.; Gulyaev, R.V.; Boronin, A.I.; Stonkus, O.A.; Zaikovskii, V.I. Role of the support in the formation of the properties of a Pd/Al₂O₃ catalyst for the low-temperature oxidation of carbon monoxide. *Kinet. Catal.* **2014**, *55*, 748–762. [[CrossRef](#)]
45. Wertheim, G.K. Core-Electron Binding Energies in Free and Supported Metal Clusters. *Z. Phys. B Condens. Matter* **1987**, *66*, 53–63. [[CrossRef](#)]
46. Gao, D.; Zhang, C.; Wang, S.; Yuan, Z.; Wang, S. Catalytic activity of Pd/Al₂O₃ toward the combustion of methane. *Catal. Commun.* **2008**, *9*, 2583–2587. [[CrossRef](#)]
47. Zhou, S.; Hao, G.; Zhou, X.; Jiang, W.; Wang, T.; Zhang, N.; Yu, L. One-pot synthesis of robust superhydrophobic, functionalized graphene/polyurethane sponge for effective continuous oil–water separation. *Chem. Eng. J.* **2016**, *302*, 155–162. [[CrossRef](#)]
48. Zhou, J.-H.; Sui, Z.-J.; Zhu, J.; Li, P.; Chen, D.; Dai, Y.-C.; Yuan, W.-K. Characterization of surface oxygen complexes on carbon nanofibers by TPD, XPS and FT-IR. *Carbon* **2007**, *45*, 785–796. [[CrossRef](#)]
49. Zhu, J.; Xiong, Z.; Zheng, J.; Luo, Z.; Zhu, G.; Xiao, C.; Meng, Z.; Li, Y. Nitrogen-doped graphite encapsulated Fe/Fe₃C nanoparticles and carbon black for enhanced performance towards oxygen reduction. *J. Mater. Sci. Technol.* **2019**, *35*, 2543–2551. [[CrossRef](#)]
50. Zhang, L.; Li, Y.; Zhang, L.; Li, D.-W.; Karpuzov, D.; Long, Y.-T. Electrocatalytic Oxidation of NADH on Graphene Oxide and Reduced Graphene Oxide Modified Screen-Printed Electrode. *Int. J. Electrochem. Sci.* **2011**, *6*, 819–829.
51. Ye, W.; Li, X.; Zhu, H.; Wang, X.; Wang, S.; Wang, H.; Sun, R. Green fabrication of cellulose/graphene composite in ionic liquid and its electrochemical and photothermal properties. *Chem. Eng. J.* **2016**, *299*, 45–55. [[CrossRef](#)]
52. Jones, C.; Sammann, E. Effect of low power plasmas on carbon fibre surfaces. *Carbon* **1990**, *28*, 509–514. [[CrossRef](#)]
53. Mangun, C.L.; Benak, K.R.; Economy, J.; Foster, K.L. Surface chemistry, pore sizes and adsorption properties of activated carbon fibers and precursors treated with ammonia. *Carbon* **2001**, *39*, 1809–1820. [[CrossRef](#)]
54. Jansen, R.J.J.; Van Bekkum, H. XPS of nitrogen-containing by thermal treatment with ammonia or hydrogen cyanide and functional groups on activated carbon. *Carbon* **1995**, *33*, 1021–1027. [[CrossRef](#)]
55. Fraga, M.A.; Jordão, E.; Mendes, M.J.; Freitas, M.M.A.; Faria, J.L.; Figueiredo, J.L. Properties of carbon-supported platinum catalysts: Role of carbon surface sites. *J. Catal.* **2002**, *209*, 355–364. [[CrossRef](#)]
56. Figueiredo, J.L.; Pereira, M.F.R. The role of surface chemistry in catalysis with carbons. *Catal. Today* **2010**, *150*, 2–7. [[CrossRef](#)]
57. Maldonado, S.; Morin, S.; Stevenson, K.J. Structure, composition, and chemical reactivity of carbon nanotubes by selective nitrogen doping. *Carbon* **2006**, *44*, 1429–1437. [[CrossRef](#)]
58. Shafeeyan, M.S.; Daud, W.M.A.W.; Houshmand, A.; Shamiri, A. A review on surface modification of activated carbon for carbon dioxide adsorption. *J. Anal. Appl. Pyrolysis* **2010**, *89*, 143–151. [[CrossRef](#)]
59. Donoewa, B.; Masoud, N.; Petra, E.; Jongh, P.E. Carbon Support Surface Effects in the Gold-Catalyzed Oxidation of 5-Hydroxymethylfurfural. *ACS Catal.* **2017**, *7*, 4581–4591. [[CrossRef](#)] [[PubMed](#)]
60. Liao, Y.T.; Chi, N.V.; Ishiguro, N.; Young, A.P.; Tsung, C.K.; Wu, K.C.W. Engineering a homogeneous alloy-oxide interface derived from metalorganic frameworks for selective oxidation of 5-hydroxymethylfurfural to 2,5-furandicarboxylic acid. *Appl. Catal. B* **2020**, *270*, 118805. [[CrossRef](#)]
61. Wang, B.; Yu, L.; Zhang, J.; Pu, Y.; Zhang, H.; Li, W. Phosphorus-doped carbon supports enhance gold-based catalysts for acetylene hydrochlorination. *RSC Adv.* **2014**, *4*, 15877–15885. [[CrossRef](#)]
62. Schade, O.; Dolcet, P.; Nefedov, A.; Huang, X.; Saraçi, E.; Wöll, C.; Grunwaldt, J. The Influence of the Gold Particle Size on the Catalytic Oxidation of 5-(Hydroxymethyl)furfural. *Catalysts* **2020**, *10*, 342. [[CrossRef](#)]
63. Kolobova, E.; Kotolevich, Y.; Pakrieva, E.G.; Mamontov, G.; Farias, M.H.; Bogdanchikova, N.; Pestryakov, A. Causes of activation and deactivation of modified nanogold catalysts during prolonged storage and redox treatments. *Molecules* **2016**, *21*, 486. [[CrossRef](#)]
64. Lahousse, C.; Cors, N.; Ruaux, V.; Grange, P.; Cellier, C. Preparation of Pd on Carbon Black by Deposition—Precipitation: Study of the Effect of the Support Functionalisation. *Stud. Surf. Sci. Catal.* **2006**, *162*, 601–608. [[CrossRef](#)]
65. Campisi, S.; Ferri, D.; Villa, A.; Wang, W.; Wang, D.; Kröcher, O.; Prati, L. Selectivity Control in Palladium-Catalyzed Alcohol Oxidation through Selective Blocking of Active Sites. *J. Phys. Chem. C* **2016**, *120*, 14027–14033. [[CrossRef](#)]
66. Slizhov, Y.G.; Matveeva, T.N.; Minakova, T.S. Acid-base properties of the surface of chromatographic sorbents modified by metal acetylacetonates. *Russ. J. Phys. Chem. A* **2012**, *86*, 463–467. [[CrossRef](#)]